AUT Journal of Civil Engineering

AUT J. Civil Eng., 3(2) (2019) 157-166
DOI: 10.22060/ajce.2019.14836.5502

Determining Bearing Failure Modes of Jointed Rock Foundations Subjected to the Load of Strip Footings

M. Imani[1*], A. Fahimifar[2]

[1] Garmsar Campus, Amirkabir University of Technology, Garmsar, Iran
[2] Department of Civil and Environmental Engineering, Amirkabir University of Technology, Tehran, Iran

ABSTRACT: The main prerequisite for choosing the best method of obtaining the ultimate bearing capacity of soils or rock masses is determining the probable failure mode that can occur beneath the footing. Most available methods for determining the bearing capacity of rock masses are based on general shear failure of the rock mass. But depending on the properties of the intact rock and the joint sets, other types of failure modes including local or punching shear failure may occur. In such conditions, using relations which are based on the general shear failure is not sufficiently precise. In this study, distinct element method was applied for performing wide sensitivity analyses on different intact rock and the joint sets characteristics; the range of occurrence of failure modes was investigated. Three types of failure modes including general shear failure, local shear failure, and punching shear failure were considered under the vertical load of a strip footing. Two perpendicular joint sets were considered for the jointed rock mass and different orientation angles and spacing were also taken into account for the joint sets. The obtained results showed that the shear strength properties of the intact rock and the joint sets, the elastic modulus of the intact rock and the orientation angle and spacing of the joints have a considerable effect on the mode of failure, while the normal and shear stiffness of the joint sets do not play an important role in the failure mode.

Review History:
Received: 15 August 2018
Revised: 14 January 2019
Accepted: 14 January 2019
Available Online: 14 January 2019

Keywords:
Rock Foundations
Bearing Capacity
Failure Mode
Numerical Analysis
Distinct Element Method

1- Introduction

Determination of ultimate bearing capacity is one of the most important geotechnical issues in civil engineering projects. The key point in choosing the appropriate method for determining the bearing capacity is to distinguish the type of failure mode created under the footing. According to the recommendations of various geotechnical resources, three main failure modes can occur in the soil layers beneath the footings which comprise the general, local and punching shear failure. Based on these three failure modes, different methods were developed by researchers to determine the bearing capacity of soils. Most of the available methods for determining the bearing capacity of soils are based on the general shear failure mode [1-5], while few studies are existed based on the local and punching shear failure [6-10]. But the main problem in selecting the most appropriate method for bearing capacity is distinguishing the failure mechanism which occurs in each specific soil bedding. Very few studies were performed in this regard, among them, the most practical available approach is that proposed by Vesic [6] in which, the failure mode was related to the relative density of the soil, embedment depth and the dimensions of the footing.

Corresponding author, E-mail: imani@aut.ac.ir

In comparison to soil beddings, few studies were performed in the field of rock mass bearing capacity, most of which are based on general shear failure [11-14]. Different other failure modes and the corresponding methods for determining the bearing capacity were also presented by researchers [15-19]. Based on the literature, most available methods for calculation of bearing capacity were focused on how to determine the bearing capacity and very few of them present a separation boundary between the failure modes. In addition, due to the discontinuous nature of rock masses, it is necessary to consider the effect of discontinuities in any suggestion about the failure mode. This would impose a great difficulty in dealing with the failure modes of jointed rock foundations. Based on the available literature, this subject was not considered enough in the literature and most previous researches were performed assuming a homogenized rock medium without considering the joints explicitly. In addition, few available researches in the field of jointed rocks were performed in the scale of small laboratory specimens which cannot be a good representative of real cases. Therefore, the present paper presented a numerical solution can be considered among the pioneers in the field of failure mechanisms of jointed rock foundations subjected to loads of strip footings. In this study, it was tried to overcome the existing deficiencies in the separation boundary between

different failure modes to some extent. The aim of this research is to provide a boundary between probable failure modes considering different properties for the jointed rock masses. To this end, using the numerical distinct element method, the probable failure mode in jointed rock foundations subjected to the load of a strip footing was determined. In the performed analyses, the rock mass was assumed to contain two orthogonal joint sets with different inclination angles. Different joints spacing were considered for the rock mass and the effect of the intact rock and the joint shear strength parameters were also investigated. The boundary between different failure modes was presented in diagrams that can be used simply in practical applications. These practical cases may include distinguishing the failure mode of jointed rock masses beneath the concrete dams, bridge footings, and high rise buildings.

2- Failure Modes in Foundations

According to foundation engineering references, three main failure modes occur beneath strip footings including general, local and punching shear failure. As shown in Figure 1a, in the general shear failure, a failure flow begins from beneath the footing, extended to the lateral sides of the footing and ultimately reaches the ground surface. In such a condition, a sudden change may be observed in the load-settlement curve of the foundation. In some conditions, this curve may reach to a certain asymptotic line that the load value corresponding to this line can be attributed as ultimate bearing capacity.

In the local failure mode, increasing the footing load results in increasing the settlement of the underlying strata. In this case, a shear flow begins from beneath the footing but slowly extends to the footing sides (solid lines in Figure 1b). On the obtained load-settlement curve, the stress that causes the shear failure surfaces to develop to the sides of the footing is called the initial failure load, $q_{u(1)}$. After that, a large settlement is required to reach the failure surfaces to the ground level (dashed lines in Figure 1b). The stress corresponding to this condition is considered as the ultimate bearing capacity that is shown with q_u in Figure 1b. If the footing stress exceeds this value, a significant increase in settlement will occur.

As shown in Figure 1c, in the punching shear failure, only the soil or rock under the footing will be affected by the footing load and the surrounding area will be unchanged. In this case, large settlements occur under the footing. The load-settlement curve for such a condition is usually a flat line or a line with a slight curvature, which does not show any sudden change in the settlement. In soil beddings, this type of failure is usually developed in loose soils with high compressibility. However, according to the European standard [20], in rock foundations, this type of failure may occur in high strength rock masses. In such a case, the settlement increases gradually with increasing the footing load, but no shear flow extends to the sides of the footing and the ground surface. Of course, if the loading of the footing continues to very large values, then the failure surfaces may eventually expand to the ground surface, however, it should be noted that such a large load has never been applied in practice. In this type of failure, the bearing capacity of the rock mass is usually determined based on the settlement criterion. According to [21-23], in soil beddings, punching failure usually occurs in a settlement approximately equal to 10% of the footing width. So the ultimate bearing capacity is the footing pressure corresponding to the settlement equal to 10% of the footing width. This criterion was confirmed by Maghous et al. [24] for the rock masses containing one joint set and by Imani et al. [25] for the rock masses containing two joint sets. Therefore, if the settlement of the rock foundation reaches 10% of the footing width, while no asymptotic line can be found in the load-settlement curve, the footing pressure corresponding to the settlement of 10% of the footing width should be selected as the ultimate bearing capacity. This method of obtaining the bearing capacity was named as the 0.1B method in which, B is the footing width.

Different methods are available in the literature for obtaining the bearing capacity. The best method should be selected according to the probable failure mode. The most important method in this regard was proposed by Vesic [6] which is applicable to soil beddings. As can be seen in Figure 2, the probable failure mode can be obtained knowing the relative density of soil (D_r), embedment depth of the footing (D_f) and factor B* which can be obtained using Equation 1:

$$B^* = \frac{2BL}{B+L} \tag{1}$$

where B and L are the width and length of the footing, respectively. Having such a reference in the field of rock foundations can be very useful in selecting the best method of bearing capacity determination for practical applications. In the present paper, very simple and useful design charts were presented that can be applied in practical engineering projects which deal with the problem of the bearing capacity of jointed rock foundations. These design charts can be used for jointed rock masses containing two orthogonal joint sets in which, various spacing, inclination, and mechanical properties were considered for the joint sets.

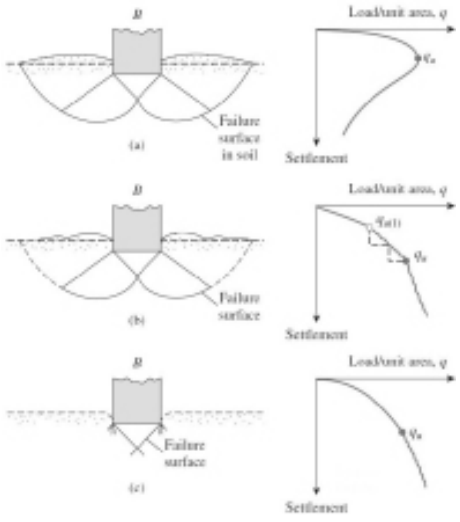

Figure 1. Types of bearing capacity failure modes in foundations: (a) general shear failure, (b) local shear failure and (c) punching shear failure [6]

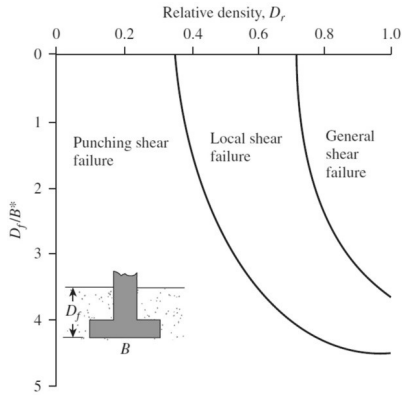

Figure 2. Modes of foundation failure in sand [6]

3- Numerical analysis of failure modes in rock foundations

3- 1- Method of analysis

According to the previous section of this paper, given the form of development of the failure surfaces under the footing and the shape of the load-settlement curve, the failure modes of the rock foundations subjected to the footing load were anticipated. In the present study, the UDEC program which is based on the distinct element method was applied for this purpose. After defining the boundary conditions and assigning material properties, the models have been implemented to achieve the initial equilibrium. Then, by ignoring the displacements developed by the initial equilibrium, the incremental loading of the footing was applied to the model top boundary and the settlement below the center of the footing was recorded. Then, the footing pressure versus the corresponding settlement was depicted in a diagram based on which and by considering the shape of displacement vectors beneath the footing, the type of failure mode was obtained. There are two general methods for drawing the load-settlement curve which are stress-controlled and settlement-controlled methods; the latter was applied in the current study. In this method, an incremental displacement was applied to the ground surface and the corresponding pressure accumulated in the rock mass grids exactly beneath the footing was recorded. Then, using the pressure and the corresponding settlement data, the curve can be drawn easily. This procedure was programmed in UDEC using the special feature of the software called FISH programming.

3- 2- Verification

In order to verify the program written for recording the load-settlement curve and the corresponding ultimate bearing capacity, a classical problem of soil bearing capacity was investigated here. This problem is determination of the bearing capacity of a cohesive soil subjected to the vertical load of a strip footing with 1 meter width. Ignoring the weight of the soil mass, Table 1 shows the assumed properties for the soil:

Table 1. Soil parameters used for verification

Parameter	Value
E (kPa)	26000
ν	0.3
c (kPa)	10
φ (degree)	0

where E is the elastic modulus, ν is the Poisson's ratio, c is the cohesion and φ is the friction angle of the soil. The bearing capacity of such a cohesive soil can easily be determined using the famous method of Terzaghi [7], which is as follows:

$$q = cN_c + qN_q + \frac{1}{2}\gamma BN_\gamma = c \times 5.14 + 0 + 0 = 10 \times 5.14 = 51.4\,kPa \quad (2)$$

where q is the surcharge pressure, γ is the density of the soil and N_c, N_q and N_γ are the bearing capacity coefficients which their values can be simply obtained from the available foundation engineering references. The parameters assumed in Table 1 and also the Equation 2 are valid for the general shear failure mode. A numerical model of the problem was also constructed in UDEC software. Because of the symmetry, only half of the footing and underlying soil were modeled. Figure 3 shows the displacement vectors of the soil body beneath the footing and Figure 4 shows the corresponding load-settlement curve. In Figure 4, drawing an asymptotic line to the final horizontal part of the curve results in an ultimate bearing capacity approximately equal to 51000 Pascal (51 kPa) which is in a good agreement with the Terzaghi [7] method.

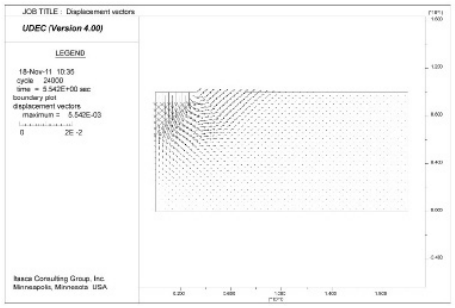

Figure 3. Displacement vectors obtained from the numerical analysis by UDEC

In addition, Terzaghi method (Equation 2) was proposed based on the general shear failure mode. The displacement vectors shown in Figure 3 were also extended from beneath the footing to the surrounding ground surface. In addition, according to Figure 4, the load-settlement curve has also been asymptote to a certain amount of load, which indicates the incidence of a general shear failure mode.

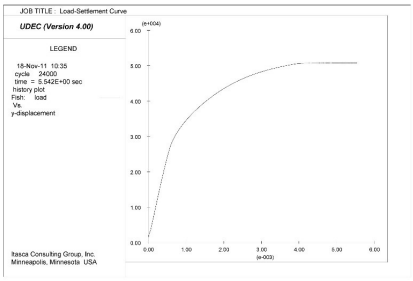

Figure 4. Load-settlement curve obtained from the numerical analysis by UDEC

3- 3- Determination of the range of occurrence of each failure mode

The type of failure mode depends on the characteristics of the intact part of the rock mass and the joint sets, as well as the orientation angle and spacing of the joints. In determining the range of occurrence of the failure mode, laboratory and field tests are very appropriate; however, performing them for each engineering project is very difficult and costly. Therefore, having some simple charts that can be used to determine the type of failure mode in the early phases of the projects will significantly be useful for engineers. Using the numerical analyses performed in this section, a general estimation of the type of probable failure mode was obtained. The analyses carried out in this section cover a wide range of rock mass properties. The indices i and j represent the intact rock and the joint sets, respectively.

As previously noted, in punching failure, before the failure surfaces are developed to the ground surface, very large settlements are created underneath the footing, which practically bring the bedrock mass to its ultimate state. In such a case, the punching failure occurs before other types of failure (i.e. general shear failure in which, the failure surfaces reach the ground level). Therefore, the priority of each failure mode should be considered. If a large settlement (say 0.1B) occurs prior to the load-settlement curve reaches an asymptotic line, a punching failure will occur in the bedrock mass prior to the general failure. Therefore, in this research, two criteria were used to detect the failure mode that was occurred in the problem. The first one is the investigation of how the failure surfaces develop in the rock bedding (extended to the surface of the ground or bounded under the footing), and the latter is the determination of the ultimate bearing capacity based on the 0.1B method or the asymptotic value to load-settlement curve, which yields the lower ultimate load. In the cases that the 0.1B method resulted in lower bearing capacity, the failure mode was distinguished as the punching or local shear failure. The difference between these two modes is that in local shear failure, the load-settlement curve approximately reaches an asymptotic line in very large settlements, while in the punching failure the curve continues to increase in an approximately linear manner. In the cases that the bearing capacity corresponding to the asymptotic line to the load-settlement curve was lower than that obtained from the 0.1B method, the failure mode was selected as the general shear failure.

3- 4- Numerical modeling hypotheses

Several numerical models were developed to determine the range of occurrence of each failure mode, some of which were schematically presented in Figure 5. Using Equation 3, the spacing of the joints was considered by a dimensionless factor, named "Spacing Ratio" (SR) that was initially proposed by [26]:

$$SR = B\sum_{i=1}^{n}\frac{1}{S_i} \tag{3}$$

where B is the footing width, n is the number of the joint sets which is equal to 2 in all of the models, and S_i is the spacing of the i^{th} joint set. The footing load was applied in a range of one meter in the middle of the upper boundary of the model. Thus, the B value in the Equation 3 was considered equal to one meter. For example, for such a case, assuming that the spacing of each joint set is equal to 35 centimeters, using Equation 3, the SR will be equal to 5.7 (as considered in Figure 6).

To minimize the effect of the boundaries of the model on the obtained results, the model boundaries were considered at a distance at least 7 times the footing width on each side, which is more than the recommended value by literature [27], which requires a minimum of 3B. The Mohr-Coulomb failure criterion was used for the intact rock and the joints. For each model, displacement vectors and the load-settlement curve were obtained, examples of which are shown in Figures 6 to 8. In these figures, α is the orientation angle of one of the joint sets (as shown in Figure 5), c_i and c_j are the cohesion of the intact rock and the joints, respectively, φ_i and φ_j are the friction angle of the intact rock and the joints, respectively, k_n and k_s are the normal and shear stiffness of the joints, respectively and E is the intact rock elastic modulus. According to Figure 6, the displacement vectors are concentrated underneath the footing. The load-settlement curve is also incremental and there is no considerable slope reduction in order to asymptote to some magnitude of the load. Consequently, the failure mode of this case was considered as punching shear failure.

Moreover, it is clear from Figure 7 that by increasing the settlement, the displacement vectors are gradually developing to the ground surface and the load-settlement curve is also becoming asymptote to a specific load. Nevertheless, the load to which the curve becomes asymptote is larger than the load corresponding to the settlement equal to 0.1B. Therefore, the failure mode was considered as the local shear failure. Based on Figure 8, the displacement vectors were developed to the sides of the footing and reached the surface of the ground. The load-settlement curve has also been asymptote to a certain load whose value is approximately equal to the load corresponding to the settlement equal to 0.1B. Thus, the failure mode corresponding to this mode can be attributed to the general shear failure.

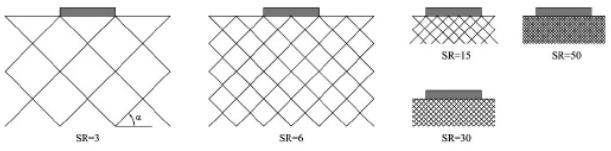

Figure 5. Schematic representation of some of the jointed rock foundation models

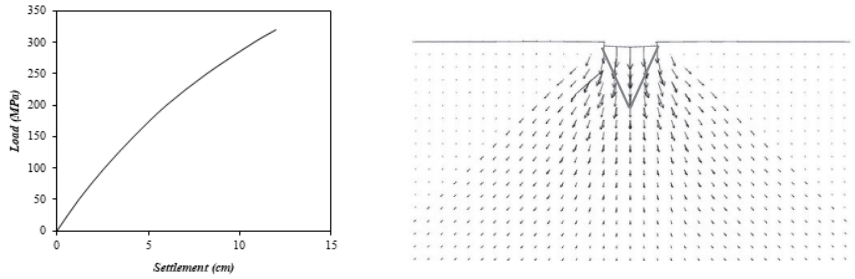

(a) Load-Settlement curve (b) Displacement vectors

Figure 6. Load-settlement curve and displacement vectors of the rock foundation for the case of α=45°, SR=5.7, c_i=25 MPa, c_j=2.5 MPa, $\varphi_i=\varphi_j$=35°, k_n= 100 GPa/m, k_s=50 GPa/m and E=15 GPa

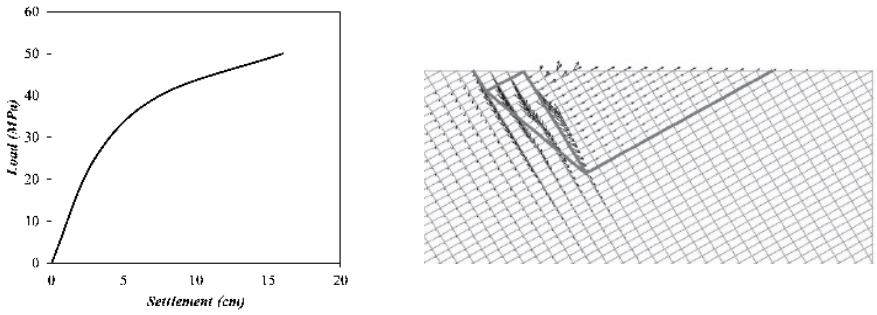

(a) Load-Settlement curve (b) Displacement vectors

Figure 7. Load-settlement curve and displacement vectors of the rock foundation for the case of α=30°, SR=9.5, c_i=5 MPa, c_j=500 kPa, $\varphi_i=\varphi_j$=35°, k_n= 100 GPa/m, k_s=50 GPa/m and E=15 GPa

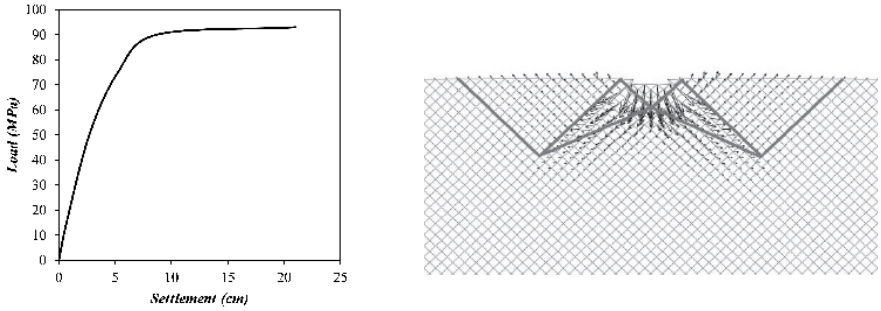

(a) Load-Settlement curve (b) Displacement vectors

Figure 8. Load-settlement curve and displacement vectors of the rock foundation for the case of α=45°, SR=8.5, ci=5 MPa, cj=500 kPa, $\varphi_i=\varphi_j$=35°, k_n= 100 GPa/m, k_s=50 GPa/m and E=15 GPa

3- 5- Parameters considered in sensitivity analyses

A wide sensitivity analyses were carried out on the most important influential parameters including cohesion and friction angle of the intact rock (c_i and φ_i, respectively) and the joint sets (c_j and φ_j, respectively), orientation and spacing ratio of the joint sets (α and SR, respectively), elastic modulus of the intact rock (E) and normal and shear stiffness of the joint sets (k_n and k_s, respectively). The selected values for these parameters were presented in Table 2. In all analyses, the density of the rock mass was considered γ=27 kN/m3 and the Poisson's ratio was assumed ν = 0.2.

Table 2. Parameters used for the sensitivity analyses

Parameter		Value
c_i (MPa)		1, 5, 15, 25
c_j/c_i		0.1, 0.5
φ_j, φ_i (degree)		(35, 25) – (35, 35) – (45, 35) – (55, 35)
k_n (GPa/m)		100
k_s (GPa/m)		50
SR	α=15°	4.9, 9.8, 19.6, 29.4, 39.1, 49
	α=30°	3.2, 6.3, 9.5, 18.9, 28.4, 41, 50.4
	α=45°	2.8, 5.7, 8.5, 19.8, 28.3, 39.6, 50.9
E (GPa)		3.7, 15

4- Results and discussion

Because of the large number of the performed analyses, in this section, only some of the outputs from the numerical analyses were presented, and the full results were figured out as design diagrams in the final subsection of the present section. It should be noted that in the diagrams presented in the following subsections, each line is the boundary between two failure modes and the small arrows drawn at each line should be used for distinguishing these two modes. The letters G, L and P beside each arrow denotes General, Local and Punching shear failure, respectively.

4- 1- Effect of shear strength parameters of the intact rock and the joint sets

The effect of shear strength parameters of the intact rock and the joint sets on the failure mode was investigated. As an example, Figure 9 shows the range of occurrence of each failure mode considering different intact rock friction angle. As it can be observed, for each intact rock friction angle, by increasing the cohesion of the intact rock, the failure mode changes from the general to the local and then to the punching failure mode. This conclusion is in accordance with the recommendation of the European standard [20], which states that by increasing the resistance (i.e. the ci) of the intact rock, the probability of the punching failure increases. Similar analyses were performed to investigate the effect of the friction angle of the joint sets. As an example, Figure 10 shows the occurrence range of each failure mode. The same results as those obtained from Figure 9 were also obtained from Figure 10.

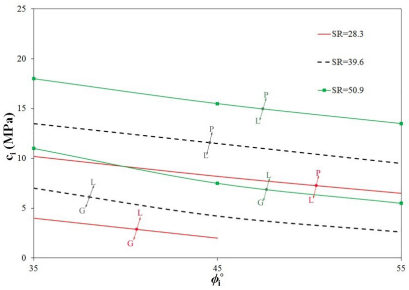

Figure 9. Effect of φ_i on the failure mode for the case of α=45°, φ_j=35°, c_j/c_i=0.1 and E=3.7 GPa

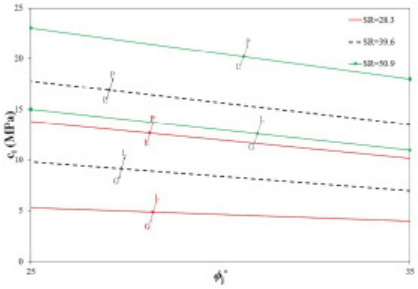

Figure 10. Effect of φ_i on the failure mode for the case of α=45°, φ_j=35°, c_j/c_i=0.1 and E=3.7 GPa

4- 2- Effect of orientation angle of the joint sets

Figure 11 shows the effect of the orientation angle of the joint sets on the type of failure mode. It can be seen that the orientation angle of the joint sets has a small effect on the failure mode. At a specific value of the intact rock cohesion, by increasing the slope of the joint sets with the horizontal direction, the failure mode may change from the punching to the local mode. Moreover, in some cases, a transform from the local mode to the general mode may occur by increasing the orientation angle.

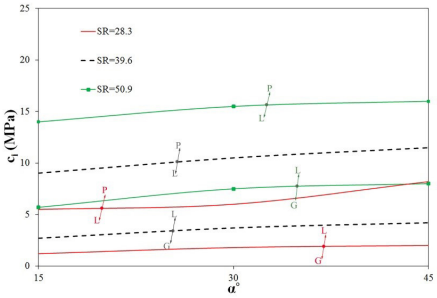

Figure 11. Effect of α on the failure mode for the case of φ_i=45°, φ_j=35°, c_j/c_i=0.1 and E=3.7 GPa

4- 3- Effect of Joint Spacing

Figure 12 shows the effect of joint spacing on the type of failure mode considering different values for the cohesion of the intact rock. For a specific intact rock cohesion, by reducing the joint spacing (increasing the SR), the failure mode transforms from the punching to the local and from the local to the general. In addition, at any specific spacing, by increasing the cohesion of the intact rock, the failure mode changes from the general to the local mode and from the local to the punching mode which is consistent with the recommendation of the European standard [20].

4- 4- Effect of elastic modulus of the intact rock

The effect of elastic modulus of the intact rock on the failure mode was depicted in Figure 13. It can be seen that for a certain value of the intact rock cohesion and a constant friction angle, by increasing the elastic modulus of the intact rock, the failure mode changes from the punching to the local and from the local to the general. In each specific elastic modulus, by increasing the

cohesion of the intact rock, the pattern of failure changes from the general to the local and from the local to the punching which is consistent with the European standard recommendation [20].

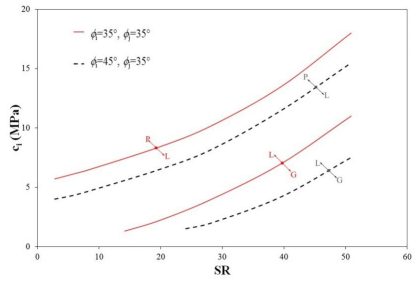

Figure 12. Effect of SR on the failure mode for the case of α=45°, c_j/c_i=0.1 and E=3.7 GPa

4- 5- The effect of the stiffness of the joint surface

For investigating the effect of normal and shear stiffness of the joint surface, stiffness values equal to one-fifth of the values used in Table 2 were also considered for the case of E = 3.7 GPa. The obtained results showed that the changing of failure modes from one to another is not affected by the normal and shear stiffness of the joint surface, which indicates the independency of the failure mode from the stiffness of the joints.

4- 6- Design Charts

The results obtained from all the analyses performed in this research were presented as design charts of Figures 14 to 16. Having the intact rock and the joint sets properties, these figures can be applied easily in practical purposes to determine the possible failure mode of jointed rock foundation subjected to the vertical load of a strip footing.

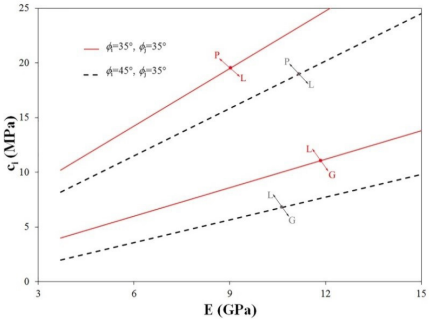

Figure 13. Effect of E on the failure mode for the case of α=45°, SR=28.3 and c_j/c_i=0.1

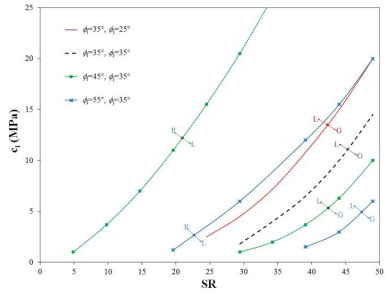

(a) E=15 GPa, c_j/c_i=0.5*

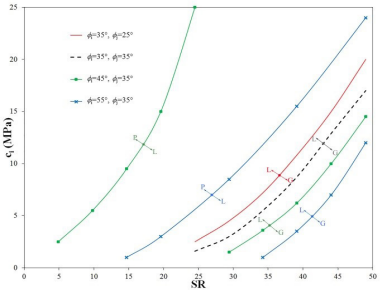

(b) E=15 GPa, c_j/c_i=0.1*

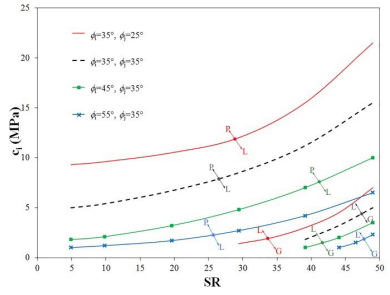

(a) E=3.7 GPa, c_j/c_i=0.5

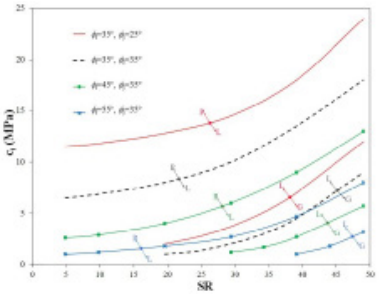

(b) E=3.7 GPa, c_j/c_i=0.1

Figure 14. Failure modes in jointed rock foundations for the case of α=15°

* For the cases of (φ_i=35°, φ_j=25°) and (φ_i=35°, φ_j=35°), punching shear failure will not occur and the corresponding curves belong to the boundary between the general and the local shear failure

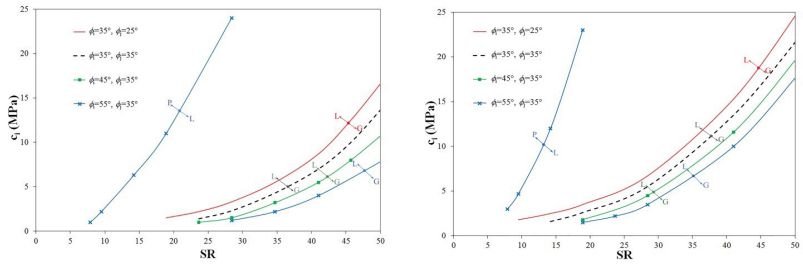

(a) E=3.7 GPa, c_j/c_i=0.5* (b) E=3.7 GPa, c_j/c_i=0.1*

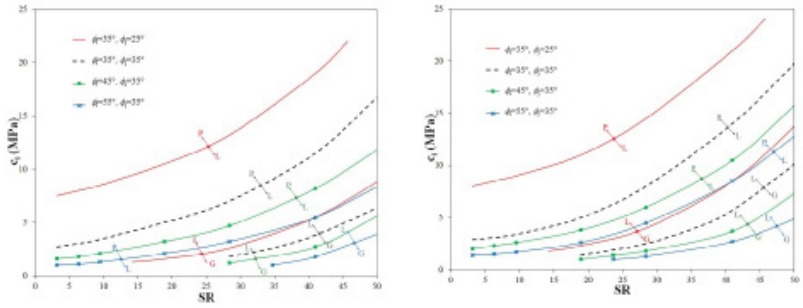

(a) E=3.7 GPa, c_j/c_i=0.5 (b) E=3.7 GPa, c_j/c_i=0.1

Figure 15. Failure modes in jointed rock foundations for the case of α=30°

* For the cases of (φ_i=35°, φ_j=25°) and (φ_i=35°, φ_j=35°) and (φ_i=45°, φ_j=35°), punching shear failure will not occur and the corresponding curves belong to the boundary between the general and the local shear failure

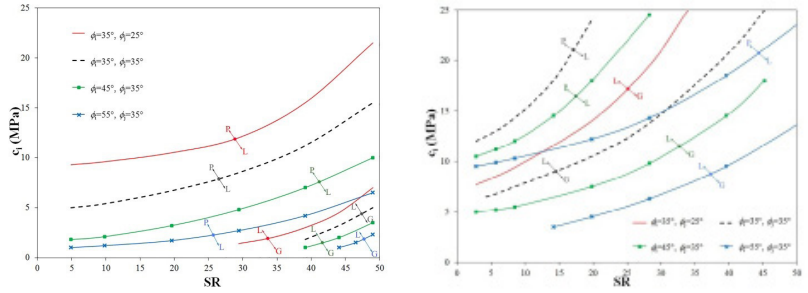

(a) E=3.7 GPa, c_j/c_i=0.5* (b) E=3.7 GPa, c_j/c_i=0.1*

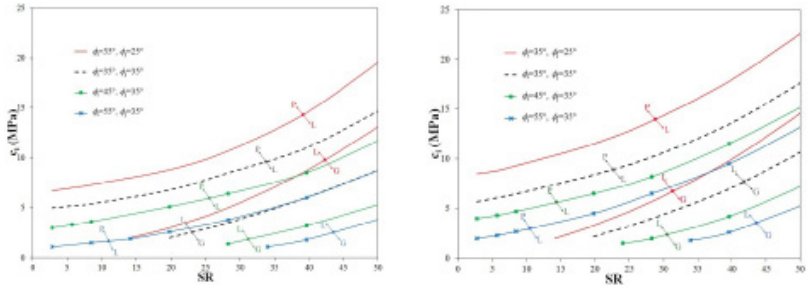

(a) E=3.7 GPa, c_j/c_i=0.5 (b) E=3.7 GPa, c_j/c_i=0.1

Figure 16. Failure modes in jointed rock foundations for the case of α=45°

* For the cases of (φ_i=35°, φ_j=25°), punching shear failure will not occur and the corresponding curves belong to the boundary between the general and the local shear failure

5- Conclusions

In this paper, three main failure modes of rock foundations including the general, local and punching failure modes were investigated and the range of occurrence of each of them was proposed. The obtained results showed that:

1. By increasing the shear strength parameters of the intact rock and the joint sets, the failure mode changes from general to local and from local to punching mode.
2. Reducing the elastic modulus of the intact rock results in changing the failure mode from punching to local and from local to general mode.
3. By increasing the orientation angle of the joint sets with the horizontal direction, the failure mode changes from punching to local and then, from local to general mode.
4. Decreasing the joint spacing results in changing the failure mode from punching to local and from local to general mode.
5. The normal and shear stiffness of the joints do not have a considerable effect on the probable failure mode.

The results obtained in this paper are only reliable for the rock beddings containing two orthogonal joint sets which are subjected to the load of strip footings. These results may be applicable for the case of small spacing of joints (i.e. large values of SR), but more researches are required in this regard. Moreover, investigating the effect of more than two joint sets and also considering other shapes for the footing can be attributed as interesting subjects for future researches.

References

[1] R.L. Michalowski, Upper-bound load estimates on square and rectangular footings, G-otechnique, 51(9) (2001) 787-798.

[2] Y.-J. Wang, J.-H. Yin, Z.-Y. Chen, Calculation of bearing capacity of a strip footing using an upper bound method, International Journal for Numerical and Analytical Methods in Geomechanics, 25(8) (2001) 841-851.

[3] A.-H. Soubra, Upper-Bound Solutions for Bearing Capacity of Foundations, Journal of Geotechnical and Geoenvironmental Engineering, 125(1) (1999) 59-68.

[4] R.L. Michalowski, L. Shi, Bearing Capacity of Footings over Two-Layer Foundation Soils, Journal of Geotechnical Engineering, 121(5) (1995) 421-428.

[5] A. Florkiewicz, Upper bound to bearing capacity of layered soils, Canadian Geotechnical Journal, 26(4) (1989) 730-736.

[6] A.S. Vesic, Analysis of Ultimate Loads of Shallow Foundations, Journal of Soil Mechanics and Foundation Division, ASCE, 99(1) (1973) 29.

[7] K. Terzaghi, Theoretical soil mechanics, John Wiley & Sons, New York, 1943.

[8] R. Amini, A. Haddad, Performance of Bucket Foundation Resting on Sand Subjected To Vertical Load, AUT Journal of Civil Engineering, (2018) -.

[9] M. KAZEMI, J. Bolouri Bazaz, Ultimate Bearing Capacity of Composite Shell Annular Foundations in Cohesionless Soil, Amirkabir Journal of Civil Engineering, 50(4) (2018) 781-792.

[10] A. Shalchi, V. Rostami, Experimental Investigation of Bearing Capacity of Strip Footing Rest on Layered Soils Next to the Geogird Reinforced Retaining Walls, Amirkabir Journal of Civil Engineering, 50(1) (2018) 211-226.

[11] M. Imani, A. Fahimifar, M. Sharifzadeh, Upper Bound Solution for the Bearing Capacity of Submerged Jointed Rock Foundations, Rock Mechanics and Rock Engineering, 45(4) (2012) 639-646.

[12] Z. Saada, S. Maghous, D. Garnier, Bearing capacity of shallow foundations on rocks obeying a modified Hoek–Brown failure criterion, Computers and Geotechnics, 35(2) (2008) 144-154.

[13] R.S. Merifield, A.V. Lyamin, S.W. Sloan, Limit analysis solutions for the bearing capacity of rock masses using the generalised Hoek–Brown criterion, International Journal of Rock Mechanics and Mining Sciences, 43(6) (2006) 920-937.

[14] X.-L. Yang, J.-H. Yin, Upper bound solution for ultimate bearing capacity with a modified Hoek–Brown failure criterion, International Journal of Rock Mechanics and Mining Sciences, 42(4) (2005) 550-560.

[15] M. Singh, K.S. Rao, Bearing Capacity of Shallow Foundations in Anisotropic Non-Hoek–Brown Rock Masses, Journal of Geotechnical and Geoenvironmental Engineering, 131(8) (2005) 1014-1023.

[16] A. Serrano, C. Olalla, Ultimate bearing capacity of an anisotropic discontinuous rock mass. Part I: Basic modes of failure, International Journal of Rock Mechanics and Mining Sciences, 35(3) (1998) 301-324.

[17] A. Serrano, C. Olalla, Ultimate bearing capacity of an anisotropic discontinuous rock massPart II: Determination procedure, International Journal of Rock Mechanics and Mining Sciences, 35(3) (1998) 325-348.

[18] Rock Foundations, in: U.A.C.o.E. Department of the Army (Ed.), Washington, DC, 1994.

[19] B. Ladanyi, Rock Failure Under Concentrated Loading, in: The 10th U.S. Symposium on Rock Mechanics (USRMS), American Rock Mechanics Association, Austin, Texas, 1968, pp. 26.

[20] R. Frank, C. Bauduin, R. Driscoll, M. Kavvadas, N. Ovesen, T. Orr, B. Schuppener, Designer's guide to EN 1997-1 Eurocode 7: Geotechnical design - General rules, (2004).

[21] A.J.a.A. Lutenegger, M.T., Bearing Capacity of Footings on Compacted Sand, in: International Conference on Case Histories in Geotechnical Engineering, University of Missouri--Rolla, St. Louis, Missouri, 1998.

[22] J.L.a.J. Briaud, P., Load Settlement Curve Method for Spread Footings on Sand, in: Speciality conference, Vertical and horizontal deformations of foundations and embankments, American Society of Civil Engineers, 1994, pp. 31.

[23] A.S. Vesic, Expansion of Cavities in Infinite Soil Mass, Journal of the Soil Mechanics and Foundations Division, (1972) 26.

[24] S. Maghous, D. Bernaud, J. Freard, D. Garnier, Elastoplastic behavior of jointed rock masses as homogenized media and finite element analysis, International Journal of Rock Mechanics and Mining Sciences, 45(8) (2008) 1273-1286.

[25] M. Imani, A. Fahimifar, M. Sharifzadeh, Bearing failure modes of rock foundations with consideration of joint spacing, Scientia Iranica, 19(6) (2012) 1411-1421.

[26] A. Serrano, C. Olalla, Allowable bearing capacity of rock foundations using a non-linear failure criterium, International Journal of Rock Mechanics and Mining Sciences & Geomechanics Abstracts, 33(4) (1996) 327-345.

[27] A. Lees, Geotechnical Finite Element Analysis.

Please cite this article using:

M. Imani, A. Fahimifar, Determining Bearing Failure Modes of Jointed Rock Foundations Subjected to the Load of Strip Footings, *AUT J. Civil Eng.*, 3(2) (2019) 157-166.

DOI: 10.22060/ajce.2019.14836.5502